Journal of Cell Science 113, 3851-3859 (2000)
Printed in Great Britain © The Company of Biologists Limited 2000
JCS1629

Antisense oligonucleotide experiments elucidate the essential role of titin in sarcomerogenesis in adult rat cardiomyocytes in long-term culture

Veronika Person[1], Sawa Kostin[1], Keisuke Suzuki[1], Siegfried Labeit[2] and Jutta Schaper[1,*]

[1]Max-Planck-Institut für Physiologische und Klinische Forschung, Abteilung für Experimentelle Kardiologie, 61231 Bad Nauheim, Germany
[2]Klinikum Mannheim, Abteilung für Anästhesiologie und Operative Intensivmedizin, 68135 Mannheim, Germany
*Author for correspondence (e-mail: j.schaper@kerckhoff.mpg.de)

Accepted 29 August; published on WWW 17 October 2000

SUMMARY

An essential role of titin as a molecular ruler in sarcomerogenesis has been frequently discussed. In this study, we tested the hypothesis that the expression of titin is a prerequisite for thick filament incorporation into sarcomeres by using an antisense oligonucleotide approach to interfere with titin translation in the de-/redifferentiation model of adult rat cardiomyocytes (ARC) in long-term culture. As a first step, the growth pattern ranging from rod shape to round and later to spreading cells and the cell surface area of ARC were quantitatively evaluated and standardized. This represents the basis for experiments interfering with sarcomere formation using three different antisense phosphorothioate oligonucleotides (S-ODN) at a dosage of 10 μM specific for titin mRNA. Presence of fluorescein labeled S-ODN in ARC indicated cellular uptake and both, antisense and random S-ODN, induced a significant increase in cell size as compared with control untreated ARC. At days 12 and 16 in culture, antisense S-ODN treatment resulted in reduced expression of titin and disturbance of myosin incorporation into sarcomeres, evident by diffuse myosin labeling and a significantly decreased area of regular myosin cross-striation (control 75%, day 12 S-ODN 20%, day 16 14%) shown by laser scanning confocal microscopy. Cellular integrity indicated by presence of α-actinin was not disturbed. These findings provide evidence for the role of titin as a template for myosin incorporation and therefore as a prerequisite for sarcomerogenesis.

Key words: Titin, Sarcomerogenesis, Oligonucleotide, Cardiomyocyte

INTRODUCTION

Titin, also called connectin (Maruyama et al., 1977; Wang et al., 1979), with a molecular mass of 3-3.7 MDa and a length of 1 μm is the largest polypeptide so far discovered. It is the third most abundant protein (8-10%) after myosin (43%) and actin (22%) in striated muscle (Yates and Greaser, 1983) and spans from the Z- to the M-line of each sarcomere directly interacting with several A-band proteins like myosin and myosin-associated proteins (Labeit et al., 1992; Obermann et al., 1997).

Titin has been implicated in a large variety of diverse functions (reviewed by Trinick and Tskhovrebova, 1999). To date, the contribution of titin to passive tension generation because of its elastic I-band segment appears to be well established (Helmes et al., 1999; Horowits, 1992; Linke et al., 1998). It has been speculated that titin acts as a structural template for thick filament assembly because titin and the myosin tail contain substructures with similar periodicities (Whiting et al., 1989). Subsequently, it was shown that the A-band region of titin contains immunoglobulin (Ig)-like and fibronectin-3 (Fn3)-like domains which are arranged in regular patterns in correlation with the ultrastructure of the thick filament (Bennett and Gautel, 1996; Labeit et al., 1992; Labeit and Kolmerer, 1995). Also, the early expression of titin may point towards contributions during myogenesis as a molecular blueprint for the sarcomeric layout, thereby directing the sequential events in sarcomere assembly (Fulton and Isaacs, 1991; Gregorio et al., 1999; Tokuyasu and Maher, 1987; Turnacioglu et al., 1997; Wang et al., 1988). Finally, titin has been implicated in determining chromosomal structure and elasticity, as well as specifying myosin II assemblies in non-muscle cells (Eilertsen et al., 1994; Machado et al., 1998).

Studies in failing human hearts with dilated cardiomyopathy show numerous morphological changes including degenerative alterations, lack of contractile elements and marked disorganization and reduction of titin. These changes suggest that defects or a lack of titin leads not only to decreased elastic properties of the sarcomere but also to disturbances in sarcomerogenesis (Hein et al., 1994).

The next logical step is to test the role of titin in living cells. Recently, we postulated that the expression of titin is the prerequisite for myosin incorporation into sarcomeres in cultured ARC (Person et al., 1999). To elucidate this hypothesis, we used an antisense approach to inhibit titin translation in ARC in long-term culture. This model has been

shown to be a suitable in vitro system to study sarcomerogenesis. Cells undergo a complex dedifferentiation (with a loss of sarcomeres resulting in quiescent cells) and redifferentiation process with de novo myofibrillogenesis and renewed contraction (for review see Mitcheson et al., 1998). In the present study, we used three different antisense phosphorothioate oligonucleotides (S-ODN) specific for titin mRNA. We provide evidence that these S-ODN are taken up by ARC and that they have a significant effect on the spatial arrangement of myosin filaments into sarcomeres implying a role for titin as a prerequisite in the sarcomerogenesis process.

MATERIALS AND METHODS

Isolation and culture of ARC

Hearts of deeply anesthetized (diethyl ether) 8-10 week old Wistar rats were excised and perfused retrogradely in a Langendorff system. Perfusion was performed at 37°C with a gas of 95% O_2/5% CO_2 supplied to the system. For the first 5 minutes, a Ca^{2+}-free perfusion buffer (pH 7.4) containing 110 mM NaCl, 2.6 mM KCl, 1.2 mM $MgSO_4$, 1.2 mM KH_2PO_4, 11 mM glucose and 10 mM HEPES was used to wash out the blood. As soon as the eluate became clear, the heart was perfused for 20 minutes with a collagenase solution that consists of perfusion buffer with 0.03% collagenase (CLS 2, Worthington Biochemical Corporation), 0.004% pronase (Boehringer), 0.005% trypsin (Sigma) and 0.04 mM $CaCl_2$. The heart was then taken off the system and the atria were removed. The ventricles were minced and the cut pieces were added to the collagenase solution containing 1.2% BSA (Sigma) for further digestion, 5 minutes at 37°C. After filtration through a nylon mesh, the cells were centrifuged at 220 rpm for 3 minutes. The pellet was washed in perfusion buffer containing 0.1 mM $CaCl_2$ and subsequently separated by a 33% Percoll (AmershamPharmacia Biotech AB) gradient. Calcium was added in three increments until a final concentration of 1.0 mM was reached. The cardiomyocytes were resuspended in culture medium (Medium 199, Sigma) enriched with 5 mM creatine, 2 mM L-carnitine, 5 mM taurine, 0.1 mM insulin, 10 mM cytosine arabinoside, 100 IU/ml penicillin/streptomycin and 10% fetal calf serum (all reagents purchased from Sigma). Cells were plated on 8-well chamber slides (Labtec, Nunc®) coated with 25 μg/ml laminin (Bekton Dickinson) in a concentration of 2×10^4 cells/well and kept in a 95% O_2/5% CO_2-incubator at 37°C. After 3 hours, the medium was replaced with fresh culture medium. Further medium changes were carried out every two days for long-term cultures. The method for evaluating cell cultures was to quantify the different cell phenotypes using immunocytochemistry and laser scanning confocal microscopy as described below.

Analysis of ARC growth pattern in long-term culture

ARC of three consecutive cultures were incubated for 28 days as described above. At nine different time points, ARC were harvested, double-stained for F-actin with TRITC conjugated phalloidin to reveal total cellular area and α-actinin, myosin, titin or myomesin to show sarcomeric integrity and investigated with laser scanning confocal microscopy. Cells were divided into following groups according to their shapes and sizes: rod-shaped, rounded and cells with total cellular areas of 500-6000 μm^2, 6001-12000 μm^2 and >12000 μm^2 (LEICA SCANware 05.1b software for determination of cellular surfaces). Of each of the four stainings and for every time point, at least 100 cardiomyocytes were counted in 10 fields of vision randomly chosen, i.e. 3600 cells per culture. Values were expressed as percentage of total cell number.

Antisense inhibition approach

Evaluation of the dose-effect relationship of antisense S-ODN revealed that 10 μmol S-ODN every 48 hours caused the most significant effects on ARC including considerably decreased titin labeling and altered thick filament formation and as well ensured long-term survival of cells exposed to this dosage. Lower dosages were less effective concerning the endpoint of this study. Dosages higher than 10 μMol showed poisoning effects evident in formation of numerous cellular vacuoles and decreased survival time. Toxic effects at higher dosages were also present with random S-ODN. Therefore, a dosage of 10 μmol S-ODN was chosen for all experiments.

Cellular uptake

Fluorescein labeled S-ODN (5′ labeled FITC-S-ODN) were directly added to the medium. ARC exposed to these S-ODN were stained for titin, myosin, and α-actinin. Cells showing fluorescent signals intracellularly were counted in the microscope.

Oligonucleotides

In three consecutive cultures, we tested three antisense S-ODN, which are complementary to titin mRNA and anneal to two different regions of the transcript. Rat titin cDNA sequences for the central I-band region were isolated from a rat skeletal muscle library (Clontech, RL3003b). A 1086 bp fragment has been deposited in EMBL data library under accession AJ401157, from which S-ODN I and II are derived. These two 21mers with average GC-content were chosen from the N2B-flanking region of the central I-band: antisense S-ODN I: 5′-AGG TGA ATT TGG CTA GGT GGC-3′ and antisense S-ODN II: 5′-GTA AGT TCC TTC GTC CTC AGG-3′. The annotations to AJ401157 indicate the location of the partial rat cDNA within the I-band titin and allow to align AJ401157 rapidly to the human titin sequences x90568 and x90569 (Labeit and Kolmerer, 1995). The fragment is coding for the Ig domains I15-I27 described by Freiburg et al. (Freiburg et al., 2000). Antisense S-ODN I corresponds to the Ig domain I27 and antisense S-ODN II to I15. A third antisense S-ODN to the rat titin was designed from EMBL data library: Accession L 38717 (Jin, 1995). ODN AS III: 5′-GAC CGT TGC AGG GGC AGA CAT-3′ codes for Ig/FN3 domains within the A-I-junction region of titin (Fig. 1).

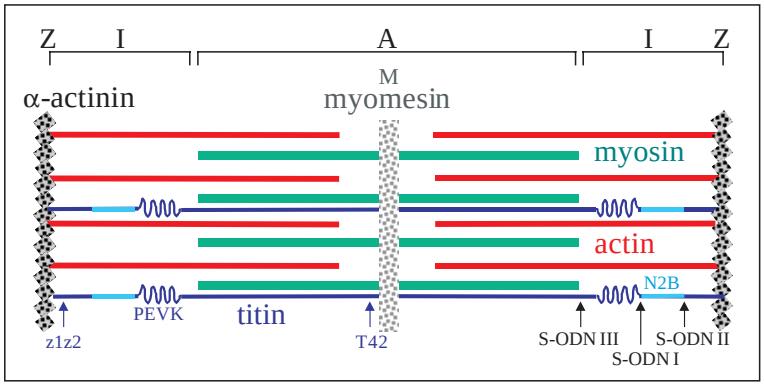

Fig. 1. Structure of a sarcomere. Schematic drawing of a half-sarcomere in which the proteins investigated are registered. T42 and z1z2 are both titin antibodies from different epitopes. Furthermore, the main parts of titin are shown: A-band titin and the elastic I-band region with two of its unique sequences, the N2B and PEVK regions. The antisense oligonucleotides S-ODN I-III are listed at their positions where they presumably inhibit translation. S-ODN I and II flank the N2B region, S-ODN III is located at the A-I-junction.

Table 1. Protocol of S-ODN treatment

Day	0	3h	1	2	3	4	5	6	7	8	9	10	11	12	13	14	15	16
Med. change*		×		×			×		×		×		×		×		×	
10 μmol S-ODN							×		×		×		×		×		×	
Investigation										×				×				×

*Med. change, medium change.

Cells of one isolation were divided into three groups to separately investigate the effects of these different S-ODN. They were cultured according to the scheme in Table 1 and S-ODN were directly added to the culture medium. Cells either treated with random S-ODN (RD I, II or III) or untreated cells served as controls. Random S-ODN were composed of the same base composition like the antisense S-ODN, but in a random order. ARC were stained for titin, myosin, α-actinin, and for F-actin using phalloidin.

Quantitative analysis of S-ODN effects

Incorporation of myosin filaments in sarcomeres results in a regular cross-stration pattern. Inhibition of the incorporation process by antisense S-ODN was the endpoint of the present study. Therefore, the area of myosin cross-striation was determined as percentage of the whole cellular area of 40 cells of each group (either antisense S-ODN treated, random S-ODN treated or untreated cells) on day 12 and 16 was determined. Ten fields of vision (objective ×40) were randomly chosen and 4 cells in each field fulfilling our criteria (spread >1000 μm^2, phalloidin (F-actin) positive, presence of myosin in cross-striated pattern) were investigated using LEICA SCANware 05.1b software. The results of the different groups were compared.

Immunocytochemistry

Cells were fixed with 4% paraformaldehyde (Merck) for 5 minutes and permeabilized for 25 minutes by using 0.05% Triton-X (Sigma) in PBS, followed by 15 minutes of 0.1% BSA. Furthermore, cardiomyocytes were exposed to the first antibody for 18 hours at 4°C (Table 2), to the second antibody for 3 hours and in the case of biotinylated secondary antibodies to Cy-2 conjugated streptavidin for 2 hours, all at room temperature. In the experiment using 5′ labeled FITC-S-ODN, cells were incubated with primary antibodies from mice or rabbits (Table 2) followed by goat anti-mouse antiserum conjugated with rhodamine (Jackson ImmunoResearch) or donkey anti-rabbit antiserum conjugated with Cy-3 (Chemicon). In double-labeling experiments, TRITC-conjugated phalloidin (Sigma) for F-actin staining was used simultaneously with the second antibody, which was either biotinylated donkey anti-mouse or donkey anti-rabbit antisera (Dianova) followed by Cy-2-conjugated streptavidin (Rockland). Between all steps, cells were washed 3 times for 3 minutes with PBS (pH 7.4). Slides were mounted with Mowiol (Hoechst). Omission of the primary antibody served as negative control for this technique.

Confocal microscopy

Cells were examined using laser scanning confocal microscopy (LEICA TCS 4D or LEICA TCS SP). Series of confocal sections (0.5-1 μm interval) were taken through the cardiomyocytes for consecutive three-dimensional reconstruction at a Silicon Graphics Indy workstation using 3-D multichannel image processing software ‘Imaris’ (Bitplane).

Statistical analysis

Analysis of the data was performed using either ANOVA and subsequent Bonferroni’s Multiple Comparison Test or Kruskal-Wallis Test with subsequent multiple comparisons by Dunn’s Test. Differences between groups were considered significant at $P<0.05$.

Table 2. Primary antibodies

Name	Clone	Host	Conc*	Company
α-Actinin	EA-53	Mouse	1:200	Sigma
Titin	T42	Mouse	1:5	Provided by Prof. Fürst
Titin	Anti-Z1-Z2	Rabbit	1:10	Provided by Prof. Labeit
Myomesin	B4	Mouse	1:5	Provided by Prof. Eppenberger
Myosin	NOQ7.5.4D	Mouse	1:250	Sigma

*Conc, concentration.

RESULTS

Analysis of ARC growth and sarcomeric pattern in culture

Quantitative analysis of ARC growth

As established in the present study, as well as in many other studies (Eppenberger et al., 1987; Nag et al., 1996), ARC in culture undergo a complex de-/redifferentiation process with a distinct transformation in size and shape from the initial rod-shaped structure to a flat polygonal phenotype with numerous new sarcomeres. Fig. 2A-F shows representative micrographs of changes in morphology of the ARC structure from the time of cell isolation and during subsequent maintainance in culture and Fig. 2G summarizes the evaluation of three consecutive cultures (mean ± s.d.). These showed a heterogeneous distribution and frequency of cellular phenotypes and were therefore quantitatively analyzed at different time points in long-term culture. Shortly after plating (day 0), there were about 80% rod-shaped cells with typically stair-like ends (Fig. 2A) and 20% round cells (data not shown), then the majority of cells started to round and at day 3 we found 13±5% rod-shaped cells with smooth ends (Fig. 2B), 24±6% rounded and 62±11% spread cells with a total cellular area of <6000 μm^2 (most of them around 500 μm^2). Rod-shaped cells disappeared after 5 days with the exception of some dead rod-shaped cells, the so-called second layer cells (Fig. 2E). Due to the fact that dead cells do not stain with TRITC-conjugated phalloidin for F-actin, they could easily be distinguished from living cells. The second-layer cells persisted in this shape for 28 days when still approximately 3% were present in culture. The number of rounded cells gradually decreased until a complete disappearance was seen at day 24. The number of cells with a surface of 6000-12000 μm^2 increased from 4±3% at day 5 to 49±5% at day 28. ARC with a surface of >12000 μm^2 first appeared at day 8 at 8±1% reaching 27±3% at day 28. This evaluation served as standardization for all following experiments as described below.

Sarcomerogenesis in ARC in culture

Freshly isolated rod-shaped cells showed distinct cross-striation throughout the entire cell for the different antibodies. Fig. 2A gives an example of T42 staining. At day 3, rod-shaped cells

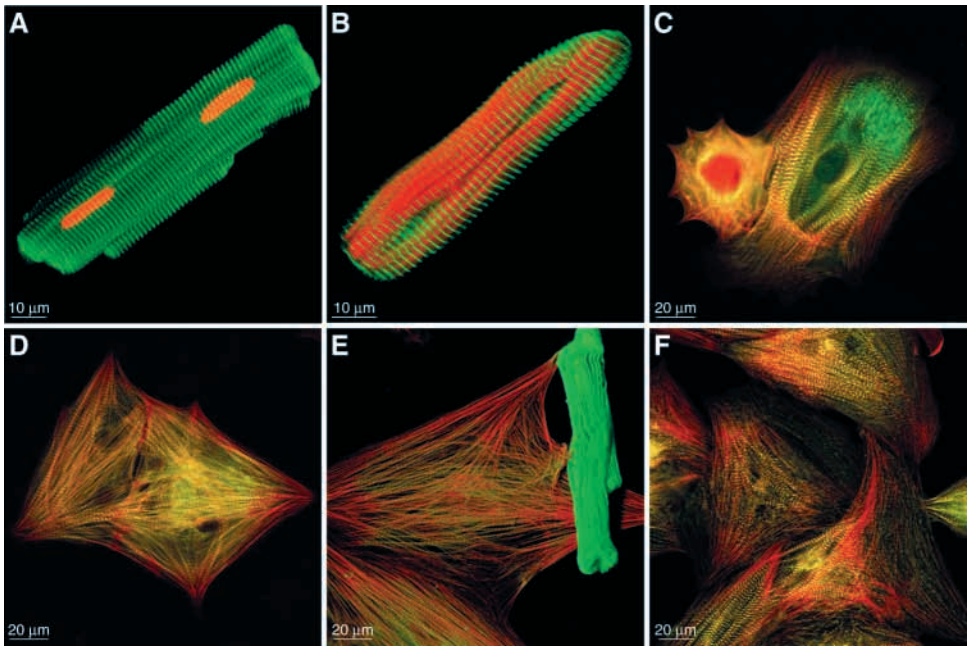

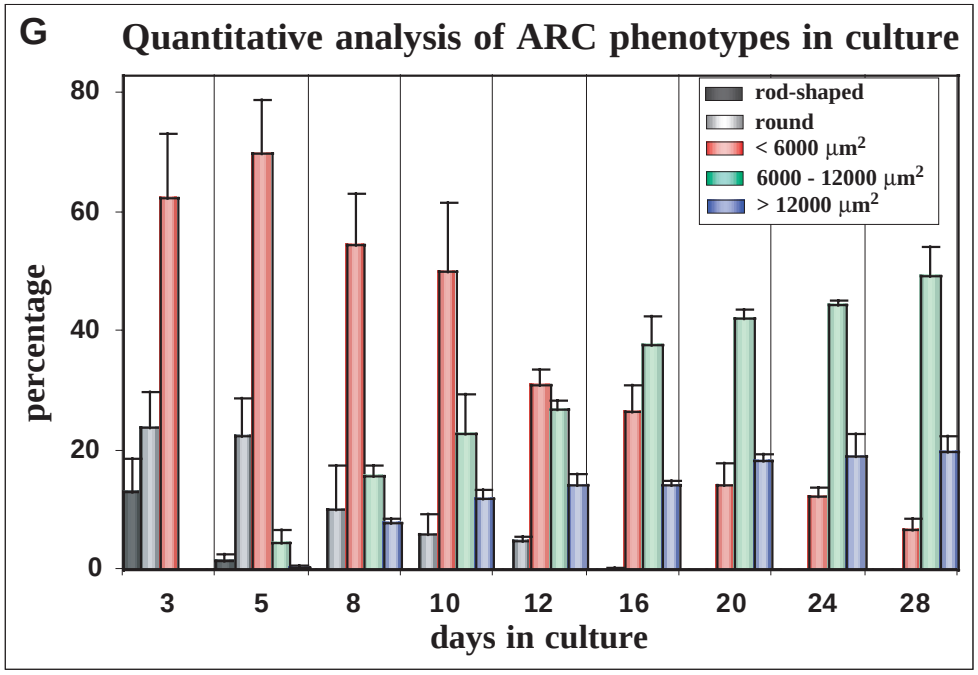

Fig. 2. Representative confocal images showing the changes in ARC phenotype and quantitative analysis of ARC in long-term cultures. Different sarcomeric proteins are stained in green. In picture A, the nuclei are stained red with propidium iodide and in picture B-F, F-actin is stained with TRITC-phalloidin (red). (A) Freshly isolated (day 0) binucleated myocyte with a characteristic rod-shaped form and blunt ends (green: T42). (B) Rod-shaped ARC displays smooth ends at day 3 (green: T42). (C) Different patterns of cellular spreading at day 8: the left cell is rounded with a concentration of sarcomeric material in the center and a small hem of pseudopods in a circular array, the right cell is presumably elongated from the attached rod-shaped form (green: α-actinin). (D) Two spreading ARC at day 10 show intercellular contact (green: myosin). (E) Clear demonstration of the change in phenotype at day 12: on the left are two spreading ARC, on the right is a so-called second layer cell that did not stain for F-actin (green: myosin). (F) ARC showing high confluency at day 16 (green: α-actinin). (G) Quantitative analysis of ARC at different time points shows a decline in the number of rod-shaped and rounded cells and an increase of large spreading myocytes. Results are expressed as the mean ± s.d.

with the typical smooth ends still displayed a clear cross-striation throughout the whole cell (Fig. 2B). However, myofibrils of rounded cells stained as a fibroamorphous mass and only rare showed a cross-striated pattern (Fig. 2C, left cell). It is typical of this dedifferentiation phase to see a loss of myofibrils. Spreading started either from rod-shaped, in most cases, or from rounded myocytes. Redifferentiation was characterized by the formation of new sarcomeres in spreading cells. These cells showed a distinct punctate pattern of α-actinin in their extensions (Fig. 3A,B). Titin appeared in a cross-striated or punctate pattern (Fig. 3C,D) but myomesin (Fig. 3E,F) as well as myosin (Fig. 3G,H) could not be detected in these first pseudopods. It was evident that during the phase of redifferentiation, α-actinin was the first protein to appear along the already existing stress-fiber-like-structures (SFLS) and that titin as well as myosin appearance occurred later. As described in Fig. 3E,G, redifferentiation starts in the center extending to the periphery (Fig. 3A,C).

Contractility of ARC in culture

A small number of freshly isolated cells still contracted shortly after isolation but became quiescent a few hours later. Cells remained in this quiescent state until day 8 where some of them started to beat again depending on their degree of redifferentiation. At later time points (day 12 onwards), cells often contracted synchroneously due to their reestablished cell-cell contacts (intercalated disk-like structures).

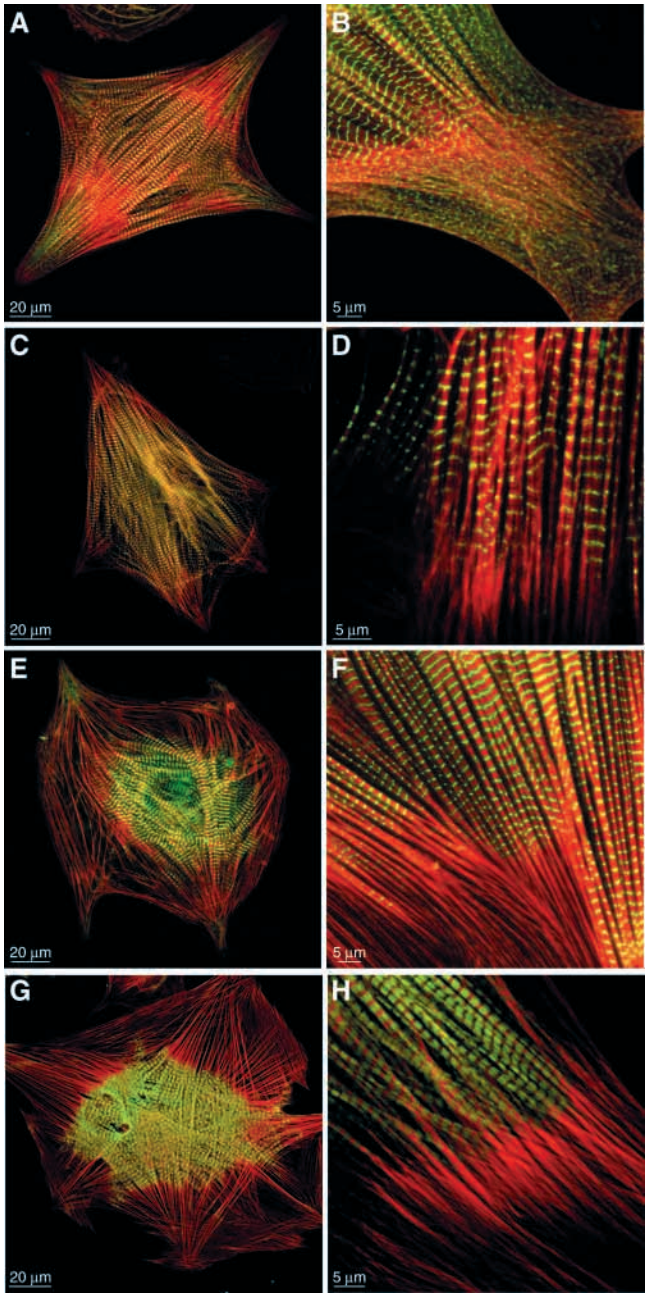

Fig. 3. Sarcomerogenesis: Confocal micrographs of ARC at day 12 stained for the different sarcomeric proteins (green) revealed an order of their appearance in the myofibril assembly with α-actinin coming first followed by titin, myomesin, and myosin. F-actin is stained red with TRITC-phalloidin. (A) Cell displaying numerous myofibrils with a distinct cross-striation for α-actinin. The extensions of this cell show a typical punctate pattern for this protein. (B) High magnification of a cell extension shows the transition of bead-like structures to the cross-striated pattern of α-actinin. (C) Titin (z1z2) is present in distinct cross-striation almost reaching the cellular periphery. (D) High magnification of the transition of striated to non-striated myofibrils reveals a punctate staining weaker than that of α-actinin. (E) Cell stained for myomesin. The cross-striated pattern is located in the center of the cell indicating that sarcomerogenesis starts in the center extending to the periphery. A punctate pattern is absent. (F) High magnification shows the almost abrupt stop of myomesin labeling on stress-fiber-like-structures. (G) Cell stained for myosin shows a similar extension of the labeling area like the myomesin stained cell. Apart from the central location of the formation of new sarcomeres, there are a few spots near the periphery where regular labeling can also be detected. (H) High magnification reveals the broad regular weaving pattern for myosin. There is no punctate staining visible. The stress-fiber-like-structures seem to serve as scaffolds in the process of myofibril assembly because the proteins appear to be anchored to these structures.

Antisense oligonucleotide approach

Cellular uptake of 5′-labeled FITC-S-ODN

FITC-S-ODN 5′ labeled entered ARC: at day 8, fluorescent signals were present in the cytoplasm of some ARC, while at day 12 and 16, the majority of ARC displayed strong positive signals of S-ODN in the cytoplasm and/or in the nuclei (Fig. 4A,B).

Effects of S-ODN treatment on ARC

In Fig. 4, the effects of S-ODN treatment on cardiomyocytes are presented. The confocal images were taken from cells that had been treated with antisense S-ODN I and random S-ODN I, respectively. The results shown in these pictures are representative for all the S-ODN (antisense and random S-ODN I-III) used in this study. α-Actinin staining serving as control for cell integrity was not affected by antisense treatment (Fig. 4A), whereas the area of titin labeling was markedly diminished by the exposure to antisense S-ODN as compared to control cells (Fig. 4C,D). The degree of incorporation of myosin filaments into sarcomeres was used as an indicator for sarcomerogenesis (myofibrillogenesis). At day 8, differences between ARC exposed to either antisense S-ODN, random S-ODN or untreated cells were absent. At day 12 and 16, control cells (untreated and cells treated with random S-ODN) showed a distinct cross-striated pattern of myosin labeling (Fig. 4E). In contrast, the majority of ARC exposed to antisense S-ODN I, II or III showed diffuse myosin labeling, whereas a cross-striated pattern of myosin was absent (Fig. 4F). However, the area of this diffuse labeling corresponded to the area of myosin cross-striation of control cells. Other cells treated with antisense S-ODN showed a very limited area of cross-striated myosin surrounded by diffuse myosin labeling. The formation of SFLS was not influenced by the antisense S-ODN treatment (Fig. 4D,F). A cross-striated pattern of F-actin was sometimes present but only in the limited area of myosin cross-striation, and mainly found in the center of cells.

Quantitative analysis of the area of myosin cross-striation in percentage of the total cellular area at day 12 showed a decrease from 75±4% in control cells to 47.6% in cells treated with S-ODN III and 20±3% in cells treated with either S-ODN I and II (Fig. 5A). At day 16, there was a further reduction of this ratio in cells exposed to the different antisense S-ODN (mean ± s.e.m.; Fig. 5B). In addition, ARC exposed to antisense S-ODN did not show any beating activity in culture after day 12 compared to random S-ODN treated and untreated cells.

Furthermore, ARC maintained in culture for 12-16 days and exposed during this time to either antisense or random S-ODN showed a significant 1.5- to 2.0-fold increase in cell size as compared to untreated cells (mean ± s.e.m.; Fig. 5C,D).

DISCUSSION

In the present paper, we tested the hypothesis that titin expression is essential for the formation of new sarcomeres in ARC in long-term culture by using an antisense oligonucleotide approach. The results showed for the first time that the interference with titin translation by antisense S-ODN consistently disturbes incorporation of myosin filaments into sarcomeres. These data provide substantial support to the proposal that titin may act as a molecular ruler directing the sequential events in sarcomerogenesis (Labeit et al., 1997) and confirm the hypothesis put forward by our group that titin is a prerequisite for myosin incorporation into sarcomeres and is essential for sarcomerogenesis. Several studies have reported effects of ODN on neonatal cardiomyocytes in culture (Shiraishi et al., 1997; Takahashi et al., 1999) but the present study is the first to describe effects of antisense ODN on sarcomerogenesis in adult rat cardiomyocytes in culture.

In the de-/redifferentiation model, cells undergo a distinct morphological transformation in size and shape by rounding and spreading from the initial rod-shaped in vivo structure to a flat polygonal phenotype (reviewed by Schaub et al., 1997). This model is suitable for the study of sarcomerogenesis, because after initial disassembly of the myofibrillar apparatus new sarcomeres develop during the redifferentiation process. Since it has been reported that this process is heterogeneous with regard to spreading and the reappearance of sarcomeric structures, we carried out a quantitative analysis of ARC phenotypes at distinct time points to reveal the typical growth pattern of these cells. The quantitative data complemented the data on the expression of specific markers of the contractile apparatus and regained beating activity indicated the onset of redifferentiation after one week in culture confirming the results of other groups (Claycomb and Palazzo, 1980; Nag et al., 1996). Our observations concerning the sarcomeric pattern of the different antibodies used in this study with α-actinin appearing first followed by titin, myosin and myomesin correspond to the findings of other groups (Nag et al., 1996; Eppenberger et al., 1988; reviewed by Fulton, 1999).

Precise quantitative determination of the myocyte growth pattern as a function of time and its standardization represent the basis for investigating the effects of ODN on sarcomerogenesis. As a first step of the antisense oligonucleotides approach, we aimed to clarify whether S-ODN are taken up by adult cardiomyocytes. Therefore, we used fluorescein labeled S-ODN that could be conspicuously observed in the cytoplasm and nuclei in the majority of ARC indicating an active transport mechanism. ODN probably enter cells through receptor-mediated endocytosis after binding to

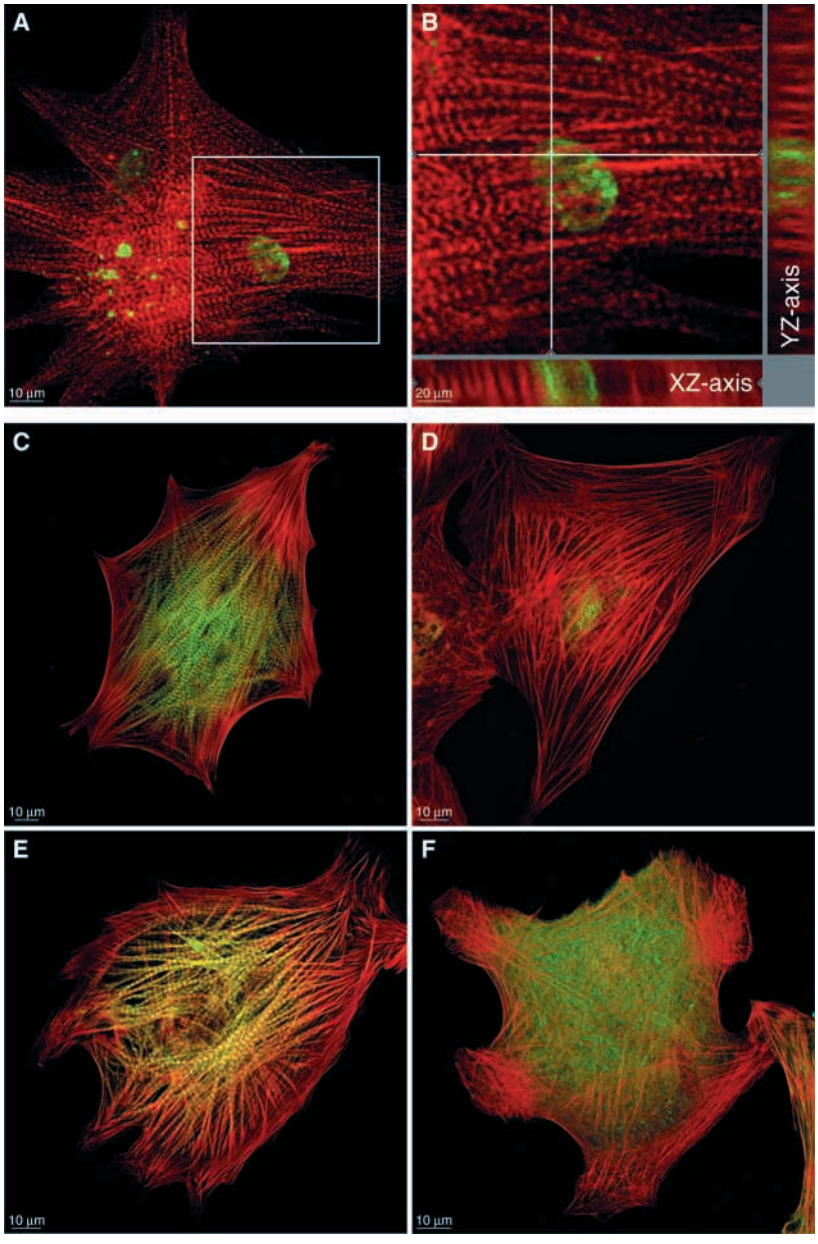

Fig. 4. Confocal images of ARC at day 12 demonstrating the uptake of S-ODN and the effects of oligonucleotide treatment on titin and on the incorporation of myosin filaments into sarcomeres. The images were taken from cells treated with antisense S-ODN I and random S-ODN I, respectively, and they are representative for all the S-ODN used (antisense and random S-ODN I-III). (A) ARC treated with FITC labeled antisense S-ODN shows uptake of S-ODN in cytoplasm and nucleus (green) and cellular integrity by α-actinin staining. (B) Subregion of Fig. A (see box). Sections (XZ- and YZ-axes) through the cell clearly demonstrate S-ODN uptake into the nucleus. (C) Control cell (treated with random S-ODN) with numerous myofibrils exhibiting a distinct cross-striated pattern for titin (z1z2) (green). F-actin is stained red with TRITC-phalloidin. (D) Cell exposed to antisense S-ODN contains only a very small area of titin (z1z2) labeling in the center. SFLS (red) appear normal. (E) Random S-ODN treated control cell displaying a regular cross-striated pattern of myosin (green). F-actin in red. (F) Cell treated with antisense S-ODN shows diffuse myosin labeling corresponding to the area of myosin cross-striation of the control cell. F-actin labeling (red) is not changed by the antisense S-ODN treatment, SFLS are visible throughout the cell.

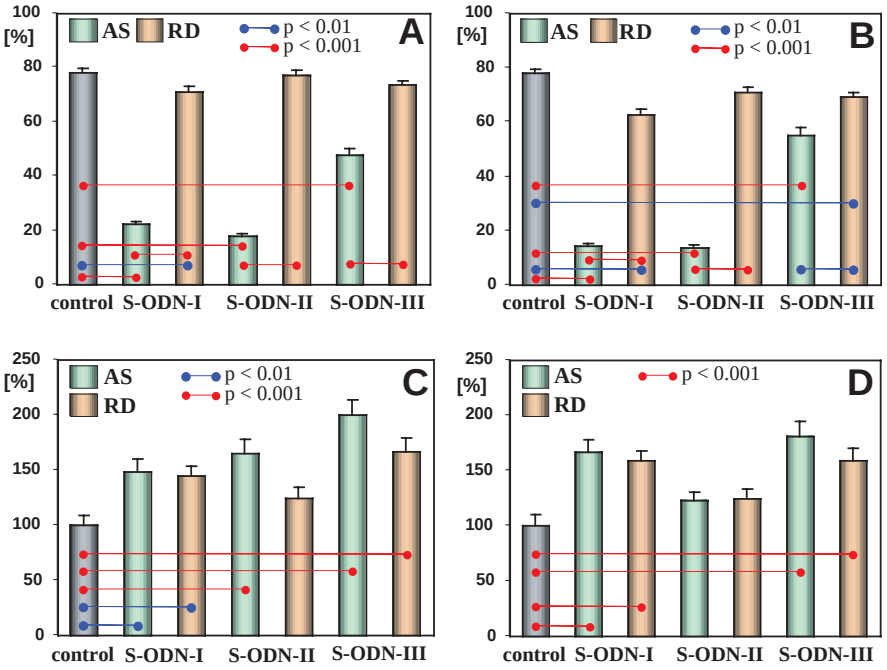

Fig. 5. Quantitiative analysis of the rate of myosin incorporation and myocyte size after treatment with S-ODN. (AS means antisense and RD random). (A,B) Significant decrease of area of myosin cross-striation as percentage of total cell area after S-ODN treatment at day 12 (A) and day 16 (B). Effects of AS S-ODN I-II were more pronounced than that of antisense AS S-ODN III, RD effects were not different from control. (C,D) Significant 1.5-to 2.0-fold increase in cellular size of cells exposed to antisense or random S-ODN compared to untreated cells at day 12 (C) and day 16 (D). All values represent the mean ± s.e.m.

cell surface proteins (Akhtar and Juliano, 1992; Loke et al., 1989). In order to improve the efficiency of ODN uptake, we used phosphorothioate ODN (S-ODN), because they have a higher resistance to nucleases (Shaw et al., 1991) and are supposed to enter cells more easily, which is confirmed by our data. ODN are able to inhibit or alter the expression of specific target genes by an antisense mechanism, i.e. to interfere with gene expression at the level of single stranded RNA (pre-mRNA or mRNA). Several mechanisms of antisense inhibition of gene expression have been discussed, e.g. inhibition of protein elongation by a steric block of the ribosome by ODN (translation arrest) (reviewed by Jansen et al., 1995). Other possibilities are targeting of the initiation area of the mRNA that prevents the constitution of the ribosomal complex or that the mRNA may become a substrate for the enzyme RNase H, which is known to cleave the mRNA strand while leaving the DNA oligonucleotide intact (reviewed by Calogero et al., 1997; Scanlon et al., 1995). Blocking the expression of titin enabled us to investigate whether this process influences synthesis and accumulation of other muscle proteins.

Incorporation of myosin filaments into sarcomeres as the endpoint of our study was chosen because myosin appearing late in sarcomerogenesis indicates the completion of this process. The late appearance of myosin was described in various studies, for example in cultured cardiomyocytes (results described in this study; Nag et al., 1996) and in skeletal muscle during embryogenesis (Furst et al., 1989).

The present S-ODN experiments resulted in a significantly decreased titin occurrence. In most of the cells, we still found a small amount of titin, the reason for this may be the low turnover of preexisting protein from the original rod-shaped cell, because antisense S-ODN suppress only de novo synthesis. In contrast, the cross-striated pattern of α-actinin serving as an indicator of cellular integrity, was not influenced by this treatment which supports the hypothesis that the assembly of I-Z-I structures occurs independently from thick filament structures (Holtzer et al., 1997). Apart from sarcomeric F-actin which was only present in the limited area of myosin cross-striation in the center of cells, the formation of SFLS was also not influenced by the antisense S-ODN treatment indicating cellular integrity and normal development of the cytoskeleton.

Myosin incorporation visible as cross-striation was minimal in antisense treated cells, but the area of diffuse myosin labeling corresponded to the area of myosin cross-striation of control cells indicating that myosin expression is undisturbed by the treatment but the filament arrangement is lacking. Cardiomyocytes without functional sarcomeres are not able to contract in cultures which confirms our findings of non-beating cells after 12 days that were exposed to antisense S-ODN. The decrease in the area of the myosin cross-striation was more pronounced after treatment with S-ODN I and II indicating that the two S-ODN from the central I-band region of titin exert a greater influence on the incorporation of myosin into sarcomeres than the S-ODN from the A-I-junction region. The reason for this discrepancy is unknown, however, the important fact is that the amount of titin protein is significantly reduced, so that we can draw conclusions on the role of titin in sarcomerogenesis using myosin incorporation in sarcomeres as the endpoint of the study. Ehler et al. (Ehler et al., 1999) postulated in their study on embryonic chicken hearts that titin functions as a ruler for sarcomere assembly as soon as its C-termini have become localized. They suggest that titin links thick filaments to complexes made up of titin, α-actinin and actin filaments that served as the first organized structures during myofibrillogenesis. This corresponds to a model proposed a decade ago in cultured embryonic cardiac muscle cells (Komiyama et al., 1993; Schultheiss et al., 1990). Our antisense inhibition experiments support this hypothesis.

Apart from the lack of myosin incorporation, we detected a 1.5- to 2-fold increase in cell size in ARC treated with both, antisense and random S-ODN. Effects of antisense and random S-ODN were similar with regard to the occurrence of hypertrophy and they were also comparable at dosages higher than 10 μM with regard to their toxic effects. The reason for

the hypertrophy observed in this study might be that S-ODN are charged polyanions and can change cell morphology and proliferation. Antisense S-ODN can also cleave non-target mRNA when used in a very high concentration. Another explanation could be that S-ODN can bind to cellular proteins in a sequence specific manner and alter cell behavior (reviewed by Stein, 1996), but since all S-ODN elicited the same effect it is rather unlikely that they bind in this way. We also have to take into consideration that cellular hypertrophy may be due to a poisoning effect. The cells, however, survived until the end of the experiment and looked intact. Hence, it is likely that oligonucleotides exert a growth stimulating effect on ARC.

The results presented in this study are important for the interpretation of structural alterations observed in human hearts that fail because of dilated cardiomyopathy characterized by lack of myofibrils and titin filaments (Hein et al., 1994; Morano et al., 1994). On the basis of these studies it was postulated that changes of the elastic sarcomeric protein titin play a major role as causative elements of structural deterioration eventually causing functional deficiencies of the heart. Our results support this proposal. If there is a lack or insufficiency in titin, sarcomerogenesis is disturbed and sarcomeres are not able to function properly finally resulting in heart failure.

In conclusion, the present data demonstrate that S-ODN are useful and effective tools to study physiological cellular processes such as myofibrillogenesis in the redifferentiation model of adult rat cardiomyocytes in long-term cultures. Interference with titin translation by antisense S-ODN treatment results in disturbance of myosin filament deposition in sarcomeres, evident by a limited area of myosin in a cross-striated pattern and/or myosin in diffuse appearance. These findings provide evidence for titin as a prerequisite for sarcomerogenesis by coordinating myosin arrangement into sarcomeres.

We thank Gunther Schuster and Gerd Stämmler for excellent computer assistance. We also thank Professor H. Eppenberger and Professor D. Fürst for their kind donations of the antibodies B4 and T42, respectively.

REFERENCES

Akhtar, S. and Juliano, R. L. (1992). Cellular uptake and intracellular fate of antisense oligonucleotides. *Trends Cell Biol.* **2**, 139-144.

Bennett, P. M. and Gautel, M. (1996). Titin domain patterns correlate with the axial disposition of myosin at the end of the thick filament. *J. Mol. Biol.* **259**, 896-903.

Calogero, A., Hospers, G. A. and Mulder, N. H. (1997). Synthetic oligonucleotides: useful molecules? A review. *Pharm. World & Sci.* **19**, 264-268.

Claycomb, W. C. and Palazzo, M. C. (1980). Culture of the terminally differentiated adult cardiac muscle cell: a light and scanning electron microscope study. *Dev. Biol.* **80**, 466-482.

Ehler, E., Rothen, B. M., Hammerle, S. P., Komiyama, M. and Perriard, J. C. (1999). Myofibrillogenesis in the developing chicken heart: assembly of Z-disk, M-line and the thick filaments. *J. Cell Sci.* **112**, 1529-1539.

Eilertsen, K. J., Kazmierski, S. T. and Keller, T. C. III (1994). Cellular titin localization in stress fibers and interaction with myosin II filaments in vitro. *J. Cell Biol.* **126**, 1201-1210.

Eppenberger, M., Hauser, I. and Eppenberger, H. M. (1987). Myofibril formation in longterm-cultures of adult rat heart cells. *Biomed. Biochim. Acta* **46**, S640-645.

Eppenberger, M. E., Hauser, I., Baechi, T., Schaub, M. C., Brunner, U. T., Dechesne, C. A. and Eppenberger, H. M. (1988). Immunocytochemical analysis of the regeneration of myofibrils in long-term cultures of adult cardiomyocytes of the rat. *Dev. Biol. (Orlando)* **130**, 1-15.

Freiburg, A., Trombitas, K., Hell, W., Cazorla, O., Fougerousse, F., Centner, T., Kolmerer, B., Witt, C., Beckmann, J. S., Gregorio, C. C. et al. (2000). Series of exon-skipping events in the elastic spring region of titin as the structural basis for myofibrillar elastic diversity. *Circ. Res.* **86**, 1114-1121.

Fulton, A. B. (1999). The elastic filament system in myogenesis. *Rev. Physiol. Biochem. Pharmacol.* **138**, 139-161.

Fulton, A. B. and Isaacs, W. B. (1991). Titin, a huge, elastic sarcomeric protein with a probable role in morphogenesis. *BioEssays* **13**, 157-161.

Furst, D. O., Osborn, M. and Weber, K. (1989). Myogenesis in the mouse embryo: differential onset of expression of myogenic proteins and the involvement of titin in myofibril assembly. *J. Cell Biol.* **109**, 517-527.

Gregorio, C. C., Granzier, H., Sorimachi, H. and Labeit, S. (1999). Muscle assembly: a titanic achievement? *Curr. Opin. Cell Biol.* **11**, 18-25.

Hein, S., Scholz, D., Fujitani, N., Rennollet, H., Brand T., Friedl, A. and Schaper, J. (1994). Altered expression of titin and contractile proteins in failing human myocardium. *J. Mol. Cell Card.* **26**, 1291-1306.

Helmes, M., Trombitas, K., Centner, T., Kellermayer, M., Labeit, S., Linke, W. A. and Granzier, H. (1999). Mechanically driven contour-length adjustment in rat cardiac titin's unique N2B sequence: titin is an adjustable spring. *Circ. Res.* **84**, 1339-1352.

Holtzer, H., Hijikata, T., Lin, Z. X., Zhang, Z. Q., Holtzer, S., Protasi, F., Franzini-Armstrong, C. and Sweeney, H. L. (1997). Independent assembly of 1.6 microns long bipolar MHC filaments and I-Z-I bodies. *Cell Struct. Funct.* **22**, 83-93.

Horowits, R. (1992). Passive force generation and titin isoforms in mammalian skeletal muscle. *Biophys. J.* **61**, 392-398.

Jansen, M., de Moor, C. H., Sussenbach, J. S. and van den Brande, J. L. (1995). Translational control of gene expression. *Ped. Res.* **37**, 681-686.

Jin, J. P. (1995). Cloned rat cardiac titin class I and class II motifs. Expression, purification, characterization, and interaction with F-actin. *J. Biol. Chem.* **270**, 6908-6916.

Komiyama, M., Kouchi, K., Maruyama, K. and Shimada, Y. (1993). Dynamics of actin and assembly of connectin (titin) during myofibrillogenesis in embryonic chick cardiac muscle cells in vitro. *Dev. Dynam.* **196**, 291-299.

Labeit, S., Gautel, M., Lakey, A. and Trinick, J. (1992). Towards a molecular understanding of titin. *EMBO J.* **11**, 1711-1716.

Labeit, S. and Kolmerer, B. (1995). Titins: giant proteins in charge of muscle ultrastructure and elasticity. *Science* **270**, 293-296.

Labeit, S., Kolmerer, B. and Linke, W. A. (1997). The giant protein titin. Emerging roles in physiology and pathophysiology. *Circ. Res.* **80**, 290-294.

Linke, W. A., Stockmeier, M. R., Ivemeyer, M., Hosser, H. and Mundel, P. (1998). Characterizing titin's I-band Ig domain region as an entropic spring. *J. Cell Sci.* **111**, 1567-1574.

Loke, S. L., Stein, C. A., Zhang, X. H., Mori, K., Nakanishi, M., Subasinghe, C., Cohen, J. S. and Neckers, L. M. (1989). Characterization of oligonucleotide transport into living cells. *Proc. Nat. Acad. Sci. USA* **86**, 3474-3478.

Machado, C., Sunkel, C. E. and Andrew, D. J. (1998). Human autoantibodies reveal titin as a chromosomal protein. *J. Cell Biol.* **141**, 321-333.

Maruyama, K., Murakami, F. and Ohashi, K. (1977). Connectin, an elastic protein of muscle. Comparative Biochemistry. *J. Biochem.* **82**, 339-345.

Mitcheson, J. S., Hancox, J. C. and Levi, A. J. (1998). Cultured adult cardiac myocytes: future applications, culture methods, morphological and electrophysiological properties. *Cardiovasc. Res.* **39**, 280-300.

Morano, I., Hadicke, K., Grom, S., Koch, A., Schwinger, R. H., Bohm, M., Bartel, S., Erdmann, E. and Krause, E. G. (1994). Titin, myosin light chains and C-protein in the developing and failing human heart. *J. Mol. Cell Cardiol.* **26**, 361-368.

Nag, A. C., Lee, M. L. and Sarkar, F. H. (1996). Remodelling of adult cardiac muscle cells in culture: dynamic process of disorganization and reorganization of myofibrils. *J. Muscle Res. Cell Motil.* **17**, 313-334.

Obermann, W. M., Gautel, M., Weber, K. and Furst, D. O. (1997). Molecular structure of the sarcomeric M band: mapping of titin and myosin binding domains in myomesin and the identification of a potential regulatory phosphorylation site in myomesin. *EMBO J.* **16**, 211-220.

Person, V., Kostin, S., Suzuki, K. and Schaper, J. (1999). Antisense experiments elucidate the essential role of titin in sarcomerogenesis. *Circulation* **100**, 1401 (Abstr).

Scanlon, K. J., Ohta, Y., Ishida, H., Kijima, H., Ohkawa, T., Kaminski, A., Tsai, J., Horng, G. and Kashani-Sabet, M. (1995). Oligonucleotide-mediated modulation of mammalian gene expression. *FASEB J.* **9**, 1288-1296.

Schaub, M. C., Hefti, M. A., Harder, B. A. and Eppenberger, H. M. (1997). Various hypertrophic stimuli induce distinct phenotypes in cardiomyocytes. *J. Mol. Med.* **75**, 901-920.

Schultheiss, T., Lin, Z. X., Lu, M. H., Murray, J., Fischman, D. A., Weber, K., Masaki, T., Imamura, M. and Holtzer, H. (1990). Differential distribution of subsets of myofibrillar proteins in cardiac nonstriated and striated myofibrils. *J. Cell Biol.* **110**, 1159-1172.

Shaw, J. P., Kent, K., Bird, J., Fishback, J. and Froehler, B. (1991). Modified deoxyoligonucleotides stable to exonuclease degradation in serum. *Nucl. Acids Res.* **19**, 747-750.

Shiraishi, I., Simpson, D. G., Carver, W., Price, R., Hirozane, T., Terracio, L. and Borg, T. K. (1997). Vinculin is an essential component for normal myofibrillar arrangement in fetal mouse cardiac myocytes. *J. Mol. Cell Cardiol.* **29**, 2041-2052.

Stein, C. A. (1996). Phosphorothioate antisense oligodeoxynucleotides: questions of specificity. *Trends Biotech.* **14**, 147-149.

Takahashi, K., Azuma, M., Huschenbett, J., Michaelis, M. L. and Azuma, J. (1999). Effects of antisense oligonucleotides to the cardiac Na^+/Ca^{2+} exchanger on calcium dynamics in cultured cardiac myocytes. *Biochem. Biophys. Res. Commun.* **260**, 117-121.

Tokuyasu, K. T. and Maher, P. A. (1987). Immunocytochemical studies of cardiac myofibrillogenesis in early chick embryos. I. Presence of immunofluorescent titin spots in premyofibril stages. *J. Cell Biol.* **105**, 2781-2793.

Trinick, J. and Tskhovrebova, L. (1999). Titin: a molecular control freak. *Trends Cell Biol* **9**, 377-380.

Turnacioglu, K. K., Mittal, B., Dabiri, G. A., Sanger, J. M. and Sanger, J. W. (1997). An N-terminal fragment of titin coupled to green fluorescent protein localizes to the Z-bands in living muscle cells: overexpression leads to myofibril disassembly. *Mol. Biol. Cell* **8**, 705-717.

Wang, K., McClure, J. and Tu, A. (1979). Titin: major myofibrillar components of striated muscle. *Proc. Nat. Acad. Sci. USA* **76**, 3698-3702.

Wang, S. M., Greaser, M. L., Schultz, E., Bulinski, J. C., Lin, J. J. and Lessard, J. L. (1988). Studies on cardiac myofibrillogenesis with antibodies to titin, actin, tropomyosin, and myosin. *J. Cell Biol.* **107**, 1075-1083.

Whiting, A., Wardale, J. and Trinick, J. (1989). Does titin regulate the length of muscle thick filaments? *J. Mol. Biol.* **205**, 263-268.

Yates, L. and Greaser, M. (1983). Quantitative determination of myosin and actin in rabbit skeletal muscle. *J. Mol. Biol.* **168**, 123-141.